

# Predicting Neurological Outcome from Electroencephalogram Dynamics in Comatose Patients after Cardiac Arrest with Deep Learning

Wei-Long Zheng†, Edilberto Amorim†, Jin Jing, Ona Wu, Mohammad Ghassemi, Jong Woo Lee, Adithya Sivaraju, Trudy Pang, Susan T. Herman, Nicolas Gaspard, Barry J. Ruijter, Marleen C. Tjepkema-Cloostermans, Jeannette Hofmeijer, Michel J. A. M. van Putten, and M. Brandon Westover\*

**Abstract—Objective:** Most cardiac arrest patients who are successfully resuscitated are initially comatose due to hypoxic-ischemic brain injury. Quantitative electroencephalography (EEG) provides valuable prognostic information. However, prior approaches largely rely on snapshots of the EEG, without taking advantage of temporal information. **Methods:** We present a recurrent deep neural network with the goal of capturing temporal dynamics from longitudinal EEG data to predict long-term neurological outcomes. We utilized a large international dataset of continuous EEG recordings from 1,038 cardiac arrest patients from seven hospitals in Europe and the US. **Poor outcome**

was defined as a Cerebral Performance Category (CPC) score of 3-5, and good outcome as CPC score 0-2 at 3 to 6-months after cardiac arrest. Model performance is evaluated using 5-fold cross validation. **Results:** The proposed approach provides predictions which improve over time, beginning from an area under the receiver operating characteristic curve (AUC-ROC) of 0.78 (95% CI: 0.72-0.81) at 12 hours, and reaching 0.88 (95% CI: 0.85-0.91) by 66 h after cardiac arrest. At 66 h, (sensitivity, specificity) points of interest on the ROC curve for predicting poor outcomes were (32,99)%, (55,95)%, and (62,90)%, (99,23)%, (95,47)%, and (90,62)%; whereas for predicting good outcome, the corresponding operating points were (17,99)%, (47,95)%, (62,90)%, (99,19)%, (95,48)%, (70,90)%. Moreover, the model provides predicted probabilities that closely match the observed frequencies of good and poor outcomes (calibration error 0.04). **Conclusions and Significance:** These findings suggest that accounting for EEG trend information can substantially improve prediction of neurologic outcomes for patients with coma following cardiac arrest.

**Index Terms—Cardiac Arrest, Coma, Deep Learning, Electroencephalogram, Outcome Prediction**

This work was supported in part by grants from NIH-NINDS (1K23NS090900, 1R01NS102190, 1R01NS102574, 1R01NS107291, T32HL007901, T90DA22759, T32EB001680), American Heart Association (postdoctoral fellowship), Neurocritical Care Society (NCS research training fellowship), Society of Critical Care Medicine-Weil research grant, Massachusetts Institute of Technology-Philips Clinician Award, and the Dutch Epilepsy Fund (Epilepsiefonds; NEF 14-18). Asterisk indicates corresponding author (M.B. Westover: mwestover@mgh.harvard.edu). W.-L. Zheng and E. Amorim contributed equally as co-first authors.

W.-L. Zheng, J. Jing, and M. B. Westover are with Department of Neurology, Massachusetts General Hospital, Harvard Medical School, Boston, MA, USA. W.-L. Zheng is also with Department of Brain and Cognitive Science, Massachusetts Institute of Technology, Cambridge, MA, USA.

E. Amorim is with Department of Neurology, University of California, San Francisco, San Francisco, CA, USA.

O. Wu is with Department of Radiology, Massachusetts General Hospital, Harvard Medical School, Boston, MA, USA.

M. Ghassemi is with Department of Computer Science and Engineering, Michigan State University, East Lansing, MI, USA, and Department of Electrical Engineering and Computer Science, Massachusetts Institute of Technology, Cambridge, MA, USA.

J. W. Lee is with Department of Neurology, Brigham and Womens Hospital, Boston, MA, USA.

A. Sivaraju is with Department of Neurology, Yale School of Medicine, New Haven, CT, USA.

T. Pang is with Department of Neurology, Beth Israel Deaconess Medical Center, Boston, MA, USA.

S. T. Herman is with Barrow Neurological Institute, Phoenix, AZ, USA.

N. Gaspard is with Department of Neurology, Universit Libre de Bruxelles, Brussels, Belgium.

B. J. Ruijter is with Department of Clinical Neurophysiology, University of Twente, Enschede, the Netherlands.

M. C. Tjepkema-Cloostermans and M. J. A. M. van Putten are with Department of Clinical Neurophysiology, University of Twente, Enschede, the Netherlands, and Departments of Neurology and Clinical Neurophysiology, Medisch Spectrum Twente, Enschede, the Netherlands.

J. Hofmeijer is with Department of Neurology, Rijnstate Hospital, Arnhem, the Netherlands, and Department of Clinical Neurophysiology, University of Twente, Enschede, the Netherlands.

## I. INTRODUCTION

CARDIAC arrest (CA) is the third leading cause of death in the US, with more than 356,000 out-of-hospital cardiac arrests (OHCA) annually [1]. Most patients surviving to hospital admission arrive in coma due to hypoxic-ischemic brain injury, and some patients are treated with targeted temperature management (TTM) to prevent further brain injury [2]. Early and accurate prediction of neurologic outcome is critical for clinical decision making and timely interventions, and several guidelines have been proposed to guide prognostication after cardiac arrest in recent decades. [3], [4] Beyond clinical examination, several ancillary tests can support outcome prediction. These include electroencephalogram (EEG) monitoring, somatosensory evoked potentials, and neuroimaging. [5]–[8] However, there is significant variability between patient presentations and brain injury patterns, making accurate prediction of outcomes challenging.

Recent literature has shown that early EEG patterns observed over the first few days following post-cardiac arrest are strongly associated with good or poor neurologic outcomes, and that the strength of these associations for some features

is time-dependent [9], [10]. For example, burst suppression, isoelectric patterns, and certain epileptiform patterns are associated with poor outcomes, with the strength of the association depending on the type and timing, and the strength of this association grows stronger 24 hours or later after cardiac arrest. [9], [11] The association between poor outcomes and burst suppression with identical bursts has been reported to be very strong [12], and isoelectric EEG patterns become strongly predictive of poor outcomes only when these persist 12 hours or later after cardiac arrest. By contrast, a continuous EEG background with normal amplitude within 12 h and preserved EEG reactivity are associated with a high likelihood of favorable outcomes. [7], [9], [12]–[16] However, due to the high volume and heterogeneity of continuous EEG data, clinicians reviewing EEG data manually are unable to provide optimal prognostic information and visual EEG review can suffer from intra- and inter-observer variability [11], [17]–[19]. Thus, despite widespread adoption of EEG monitoring in comatose cardiac arrest patients, full EEG interpretation remains challenging. In contrast, quantitative analysis of continuous EEG offers automated reproducible measurements. [20]–[22]

Although the EEG after cardiac arrest is dynamic, few studies have investigated the prognostic value of EEG trend information. If trends in EEG features carry important prognostic information, algorithms should be able to leverage these trends to make increasingly more accurate predictions with increasing duration of brain activity monitoring. However, previous algorithms have had limited ability to leverage changes across consecutive hours of EEG monitoring. Most recent studies focus on the first 24 hours after cardiac arrest [9], [23], and most prior algorithms make predictions based on isolated time windows within this early period without integrating the evolution of the EEG across time. It is unclear whether long-term EEG dynamics can be leveraged to improve the accuracy of neurologic prognostication, and it is unclear how best to aggregate information across time both within and beyond the first 24 hours.

Recent advances in machine learning (ML) can help deal with the challenges making predictors from complex data in healthcare settings [24]–[28]. ML approaches have been used to leverage EEG data to predict neurological outcomes in comatose patients after cardiac arrest. [21], [29]–[31] However, the performance of some of these algorithms did not improve monotonically with increasing duration of observation, and in fact worsened in one study including data beyond 24 h [32]. While one conclusion could be that EEG beyond the first 24 hours does not add to discrimination between good and poor outcome groups, we hypothesize that prior approaches have not made optimal use of trend information. A previous study demonstrated that a simple time-sensitive model that leverages time-varying features outperforms baseline methods that are time-insensitive when evaluated on the same dataset [31]. More recently, deep neural networks, specifically convolutional neural networks, were shown to perform best in outcome prediction at 12 and 24 hours after cardiac arrest [29]. However, these prior results have an important limitation in that the long-term trends in the EEG are not explicitly modeled. Deep neural networks with the ability to make use

of long-term trends in EEG have not yet been explored.

In this study, we develop a deep learning model for neurologic outcome prediction which leverages trend information in continuous EEG data to improve outcome prediction in patients with coma following cardiac arrest. The performance of our proposed model is evaluated on a large multi-center cardiac arrest EEG dataset (1,038 patients), with data from seven hospitals in Europe and the US. We show that performance of the proposed model exceeds that of other prior new models when evaluated in our cohort. [20], [21], [31], [32] Furthermore, we show how our models performance continuously improves with increasing duration of observation, well beyond the initial 24 hours of monitoring.

## II. MATERIALS AND METHODS

### A. Dataset

We developed deep learning models using the multi-center cardiac arrest EEG dataset of the International Cardiac Arrest EEG Consortium (ICARE) with 1,038 patients from seven hospitals in Europe and the US (Fig. 1a). The seven hospitals were Medisch Spectrum Twente (Enschede, Netherlands), Rijnstate Hospital (Arnhem, Netherlands), Erasmus Hospital (ULB, Brussels, Belgium), Brigham and Womens Hospital (BWH, Boston MA, USA), Beth Israel Deaconess Medical Center (BIDMC, Boston, MA, USA), Massachusetts General Hospital (MGH, Boston MA, USA), and Yale New Haven Hospital (YNH, New Haven, CT, USA). The cardiac arrest EEG monitoring protocols at participating institutions were initiated during hypothermia and continued upon rewarming for a total of approximately 48-72 hours. We developed an international multicenter EEG dataset (ICARE, International Cardiac Arrest EEG Consortium), to achieve a large and diverse cohort [29], [31]. The ICARE dataset contains approximately 58,000 hours of prospectively collected clinical EEG data, patient demographic information, and medical information from the time of admission up to 6 months after cardiac arrest. The study was based on a retrospective observational cohort. The research protocol was approved by the Institutional Review Boards of participating hospitals. Written informed consent was not required for this retrospective study.

Neurologic outcomes were assessed using the Cerebral Performance Category (CPC) scale (1-5) at 3 or 6 months after hospital discharge after cardiac arrest [8], [33]. Good outcome was defined as a CPC score of 1 or 2 (minimal to moderate neurologic disability), and poor outcome was defined as a CPC score of 3-5 (severe neurologic disability, persistent coma or vegetative state, or death). Four institutions (MGH, BWH, YNH, and BIDMC) assessed best CPC scores retrospectively through chart review at 6 months and one (ULB) at 3 months. In these institutions, CPC scores were not further reviewed for patients who achieved a good outcome (CPC 1-2) or died by hospital discharge [34]. Subjects discharged with a CPC of 3-4 had additional chart reviews performed to evaluate for recovery or worsening in CPC at 6 months from cardiac arrest. Less than 2% of subjects included required this review. Two institutions recorded CPC scores prospectively through phone or in-person interview for surviving patients (Medisch

TABLE I  
PATIENT CHARACTERISTICS, GROUPED BY CPC SCORES.

CPC group	CPC 1	CPC 2	CPC 3	CPC 4	CPC 5
Number of patients	303	70	31	17	617
Age (years)	57 (15)	56 (15)	66 (11)	54 (21)	62 (16)
Female gender (%)	29.04	24.29	35.48	47.06	32.25
Shockable rhythm (VFib/VT, %)	71	67	42	41	31
EEG start time (h)	17 (14)	16 (16)	16 (13)	20 (6)	20 (17)
EEG duration (h)	52 (33)	63 (44)	69 (51)	99 (60)	53 (40)
Out-of-hospital CA (N/A)*	232 (21)	50 (6)	17 (4)	14 (0)	439 (43)
TTM (N/A)*	261 (34)	61 (7)	26 (5)	11 (2)	514 (64)

VFib: ventricular fibrillation; VT: ventricular tachycardia; TTM: targeted temperature management; EEG start time (h) is relative to time of cardiac arrest. All numbers related to age and EEG expressed as mean (standard deviation). \*For the number of out-of-hospital CA patients and TTM, we didn't have all information available from different hospitals.

170 Spectrum Twente and Rijnstate Hospital). 665 out of 1038  
171 patients (64%) had a poor outcome. Patient characteristics  
172 grouped by CPC scores are summarized in Table I.

173 The inclusion criteria included non-traumatic cardiac arrest,  
174 age  $\geq 18$  years, return of spontaneous circulation (ROSC),  
175 Glasgow Coma Scale score  $\leq 8$  on admission, and manage-  
176 ment with targeted temperature management (TTM). Exclu-  
177 sion criteria were acute cerebral hemorrhage or acute cerebral  
178 infarction. The TTM protocol starts as soon as possible after  
179 admission to the emergency room or intensive care unit in  
180 participating centers with external cooling pads. Goal temper-  
181 ature (32-34 °C or 36 °C) is maintained for 24 hours, and there  
182 is gradual rewarming at 0.25-0.5 °C to 37 °C. Neuromuscular  
183 blocking agents are used as needed for shivering for all par-  
184 ticipating centers with exception of the Massachusetts General  
185 Hospital, which utilizes neuromuscular blockade continuously  
186 throughout TTM. Sedation management during TTM is done  
187 at the treating clinicians discretion. Commonly used sedatives  
188 and standard dosing ranges are propofol (25-80 mcg/kg/h),  
189 midazolam (0.1 mg/kg/h), or fentanyl (25-200 mcg/h). Only  
190 one institution (ULB) used midazolam for sedation prefer-  
191 entially, with the remaining institutions using propofol. At  
192 participating institutions, recommendations about withdrawal  
193 of life-sustaining therapies are a collaborative effort between  
194 critical care and neurology teams, following structured proto-  
195 cols. Multimodal neurological prognostication involved serial  
196 neurological examinations with a combination of continuous  
197 EEG monitoring, head CT or brain MR imaging, neuron spe-  
198 cific enolase, and somatosensory evoked potentials as deemed  
199 necessary by the treating clinicians.

## 200 B. Data Preprocessing and Feature Extraction

201 EEGs were recorded routinely with 19 electrodes according  
202 to the international 10-20 system. Recorded EEGs were hetero-  
203 geneous across hospitals in terms of channel names, sampling  
204 rates, etc. The raw data were standardized by matching channel  
205 names, applying digital bandpass filters (0.5-30 Hz), and re-  
206 sampling to 100 Hz. EEGs were re-referenced to 18 bipolar  
207 channels (Fp1-F7, F7-T3, T3-T5, T5-O1, Fp2-F8, F8-T4, T4-  
208 T6, T6-O2, Fp1-F3, F3-C3, C3-P3, P3-O1, Fp2-F4, F4-C4,  
209 C4-P4, P4-O2, Fz-Cz, Cz-Pz). We chose bipolar referencing  
210 for three main reasons: 1) to reduce artifacts such as ECG,  
211 which can contaminate the common average reference; 2)

212 because this montage is often found to be useful in clinical  
213 practice; and 3) Previous quantitative EEG analysis and  
214 modeling in cardiac arrest used bipolar channels [29], [32].

215 We identified the following typical types of artifacts for each  
216 5-s epoch: 1) abnormally high amplitude values above  $500 \mu V$ ;  
217 2) small standard deviation of the signal ( $< 0.2 \mu V$ ) for more  
218 than 2 s within the 4 second epoch; 3) overly fast amplitude  
219 change with more than  $900 \mu V$  within 0.1 s; 4) staircase-like  
220 spectral patterns (commonly caused by ICU machines such  
221 as cooling blankets or pumps). Clinical EEG recorded in the  
222 intensive care environment often contains artifacts and noise.  
223 Therefore, we developed a preprocessing pipeline to reduce  
224 the influence of artifacts and noise. The steps of the pipeline  
225 were as follows: 1) an artifact detection algorithm was used  
226 to assign an artifact indicator (0/1) to each consecutive 5-s  
227 EEG epoch (applied without overlap). 2) Signal quality was  
228 calculated as the percentage of clean epochs within each 5-  
229 min EEG segment. 3) The quality scores were then used as  
230 weights to the EEG features from each segment and the weight  
231 averaged features were used as the inputs to the models.

232 We extracted nine clinically interpretable EEG features  
233 for each bipolar channel with a sliding 5-min time window  
234 without overlapping: burst suppression ratio, Shannon entropy,  
235  $\delta$  (0.5-4 Hz),  $\theta$  (4-7 Hz),  $\alpha$  (8-15 Hz),  $\beta$  (16-31 Hz) band  
236 power,  $\alpha/\delta$  ratio, regularity, and spike frequency. The ex-  
237 tracted features were averaged over all bipolar channels to  
238 provide inputs to the machine learning models. The sequences  
239 of EEG features at each 6-h time interval were used as inputs  
240 of the time-dependent models. In cases of intermittent missing  
241 data (periods when EEG monitoring was interrupted), missing  
242 epochs were interpolated to values in the nearest available  
243 epochs.

244 Burst suppression is an EEG pattern consisting of peri-  
245 ods of depressed voltage alternating with periods of higher  
246 voltage activity. The burst suppression ratio was calculated  
247 as the percentage of time in the suppression within a 5-  
248 minute interval using a recursive variance estimation approach  
249 [35]. Epileptiform discharge detection was performed using  
250 an automated detection algorithm, SpikeNet, described in our  
251 previous work, and epileptiform discharge frequency (number  
252 of discharges / 5 mins) was the feature utilized to represent  
253 epileptiform discharges in our model. [36] Shannon entropy  
254 measures signal complexity. Regularity is a measure used

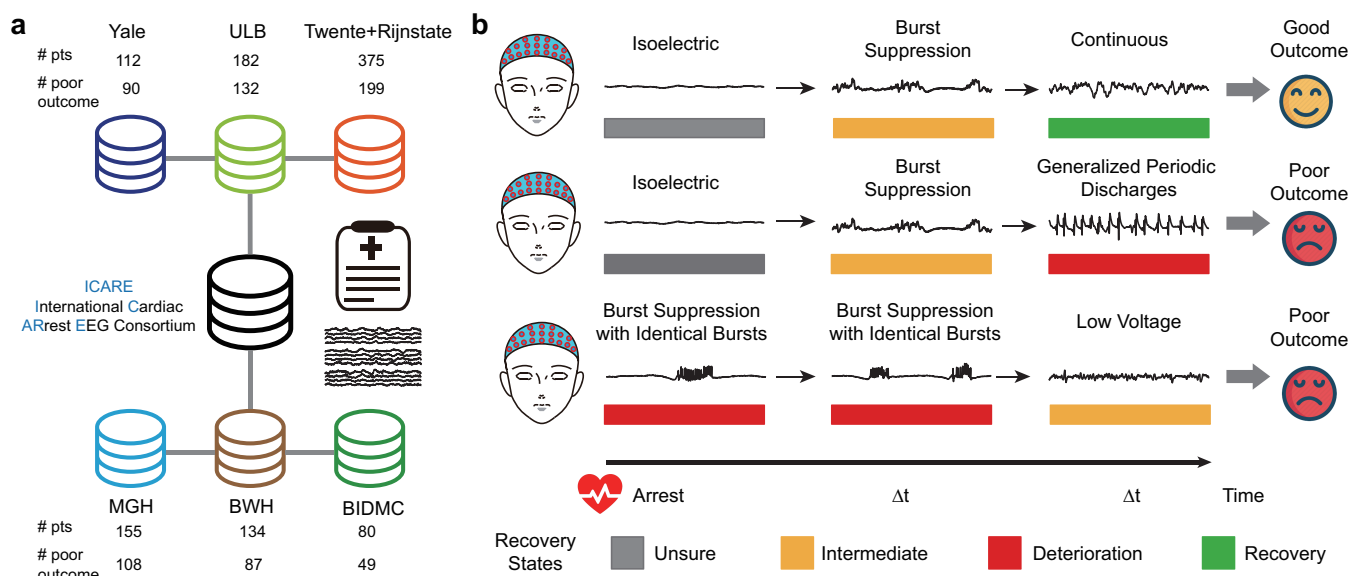


**Fig. 1.** Study framework. a, We used a large cardiac arrest EEG dataset (ICARE) from seven university-affiliated hospitals in Europe and the US to develop and externally validate the generalization of our prediction models across centers. b, Illustration of the importance of evolution over time with associations between EEG patterns and outcome after cardiac arrest. For example, a rapid transition from an isoelectric state to burst suppression to continuous activity within 12 hours after cardiac arrest usually portends good outcome. EEG patterns present at any given time might not consistently differentiate outcomes. Both the occurrence and the temporal dynamics of EEG patterns contribute to optimally predicting neurologic outcome.

in prior work to separate burst suppression patterns from continuous patterns [20]. For calculating regularity, the EEG signal was smoothed with a moving average, and the data points of smoothed signals were sorted in descending order [20]. The normalized standard deviation of the sorted signal was calculated as a feature for regularity.  $\delta$ ,  $\theta$ ,  $\alpha$ ,  $\beta$  band power, and  $\alpha/\delta$  ratio were calculated using the short time Fourier transform with Hamming windows.

### C. Model Architecture

Our approach views neurologic outcome prediction as a progressive goal, based on analysis of the evolution of brain states. The states are manifest by different characteristic EEG patterns (Fig. 1b). Prior work by us and others [31], [37] shows that some EEG patterns are strongly associated with a good or poor outcome when seen at any time, e.g., epileptiform patterns (e.g. generalized periodic discharges on a flat background or burst suppression with identical bursts), while the prognostic significance of some intermediate EEG patterns is strongly time dependent, e.g., discontinuity in the EEG [31]. We aimed to endow our outcome prediction model with the ability to capture long-term EEG dynamics to improve overall prediction performance. To achieve this, we developed a time-dependent deep learning model with bidirectional long-short time memory recurrent neural networks (Bi-LSTM).

The input sequences for this model have two components that are concatenated: 1) a mean historical feature sequence: this is obtained by averaging the sequences of feature vectors from all prior 6-hour epochs. Each such sequence contains 72 feature vectors (one from each consecutive 5-minute window), and averaging these sequences produces a single average sequence. Epochs with missing data were interpolated to

values in the nearest available epochs prior to averaging. The dimensions of this average sequence are  $9 \times 72$  (9 features in each feature vector  $\times$  72 consecutive 5-minute periods in the 6-hour epoch). This average sequence of feature vectors provides historical context for the network in which to evaluate data from the current 6-hour window. 2) A current sequence: the sequence of EEG feature vectors from the current 6-h window. The dimensions of this sequence are also  $9 \times 72$  (9 features in each vector  $\times$  72 consecutive 5-minute periods). This arrangement is illustrated in Fig. 2b.

The Bi-LSTM learns temporal dependencies between time steps in the EEG time series by forward and backward processing (Fig. 2a). LSTM introduces multiple gating mechanisms to address the vanishing gradient problem in the backpropagation through time algorithm. The hyperparameters of the neural network were tuned by cross-validation. The best network architecture consisted of four Bi-LSTM layers, three dropout layers, one fully connected layer, and a softmax layer (Fig. 2c). We used multilayered Bi-LSTMs, which mapped the input time series into multiple hidden features. The last element of the output sequence from the top-level Bi-LSTM layer was used as the input for a fully connected layer. Dropout was used during training to help avoid overfitting, and a softmax layer was used to calculate the posterior probability of neurologic outcome. Cross entropy was used as the loss function. Stochastic gradient descent with momentum (SGDM) optimizer was applied to train the deep neural networks. Training samples for the neural network consisted of 6-h EEG time blocks. The final stage of the neural network operating on each 6-hour block (NOPM, neurologic outcome prediction module) produces an estimate of the probability that the final neurologic outcome will be poor. In order to leverage information in past EEG time windows, we developed a sequence of Bi-LSTMs

319 and averaged the output probabilities to arrive at the current  
320 predicted probability of a poor outcome (Fig. 2d).

#### 321 D. Baseline Comparison

322 We compared the performance of our proposed model with  
323 state-of-the-art models on the same dataset. Previous studies  
324 found that a simpler convolutional architecture sometimes  
325 outperforms canonical recurrent networks, e.g., LSTM [38]. A  
326 recent study applied convolutional neural networks to outcome  
327 prediction and achieved better performance than previously  
328 reported predictors [29]. Therefore, we included a convo-  
329 lutional architecture called temporal convolutional network  
330 (TCN) for comparison [38]. TCN performs dilated causal  
331 convolution using multiple stacked convolutional layers. With  
332 dilated convolution, higher level convolutional layers have  
333 larger receptive fields. The TCN architecture also consists  
334 of multiple residual blocks, which allows layers to learn  
335 modifications to the identity mapping. [38] Another time-  
336 dependent model called a sequence of generalized linear  
337 models with Elastic Net regularization (SGLM with Elastic  
338 Net) was proposed recently [31]. This approach allows models  
339 operating at later time points later to consider both past  
340 and present features when making predictions. SGLM with  
341 Elastic Net can automatically select features based on  $\ell_1$  and  
342  $\ell_2$  normalization. A conventional baseline classifier, Random  
343 Forest, was evaluated to show the performance of models  
344 without time dependency.

#### 345 E. Hyperparameter Tuning

346 For Bi-LSTMs, we tuned the following hyperparameters:  
347 number of layers, number of neurons in each layer, maximal  
348 epochs. The ranges of numbers of layers and neurons were  
349 [1, 2, 3, 4] and [10, 20, 30, 40, 50], respectively. The  
350 maximal epochs were tuned in the range [50 100]. Training  
351 data were shuffled every epoch and early stopping was used.  
352 We used internal cross validation for hyperparameter tuning  
353 (training and validation sets). The best hyperparameters were  
354 determined based on the average performance in internal cross  
355 validation using an validation set (a subset of the training data).  
356 The hyperparameters in each fold were the same in internal  
357 cross validation. For TCNs, four residual blocks were used  
358 containing dilated causal convolution layers with each 170  
359 filters of size 15. The number of filters was tuned in the range  
360 [150, 250] with a step of 10. Filter size was tuned in the range  
361 [3, 15] with a step size (stride) of 2. The penalty parameter of  
362 SGLM with Elastic Net was tuned with the values of 0.5 and  
363 1. For Random Forest, the number of trees was tuned between  
364 20 and 90 with a step of 10. The best penalty parameter  $\alpha$  in  
365 SGLM with Elastic Net was 1 and the best number of trees  
366 in Random Forest was 60.

#### 367 F. Performance Evaluation Metrics

368 To quantify the stability of model performance, we used  
369 5-fold external cross validation and report average perfor-  
370 mance and 95% confidence intervals. We randomly partitioned  
371 available data into 5 folds, where 4 folds were used train

model parameters (training and validation sets in internal cross  
validation) and the remaining 1-fold was used for model  
evaluation (test set). The split of training, validation, and  
test sets was patient-independent within each of the 5 folds.  
Data from the same patients were exclusively in either in the  
training set or test set; no patient ever had data in both sets. The  
area under the receiver operating characteristic curve (AUC-  
ROC) and calibration error were used as evaluation metrics.  
Calibration error compares predicted probabilities with the  
observed event frequencies. The averages over five folds were  
calculated for comparison. The 95% confidence intervals were  
calculated using the approach of Hanley and McNeil [39],  
[40]. Statistical significance was evaluated using  $t$ -test and  $p$   
values below 0.05 were considered as statistical significance.  
We compared the sensitivity and specificity with a thresholded  
score from the models (99%, 95%, and 90%).

Due to patient privacy in multiple hospitals, the data in  
the study are not available to the publicity. The processing  
pipeline and model implementations were based on standard  
model libraries and scripts in Python and MATLAB. The  
statistical analysis code used in the study is available from  
the corresponding author on reasonable request.

### III. RESULTS

#### A. Performance Evaluation

396 We compute all performance measures for each 6-h time  
397 interval between 12-96 h after cardiac arrest. To quantify  
398 the stability of these performance measures, we perform 5-  
399 fold cross validation. The reported AUC-ROC and calibra-  
400 tion errors are averages over the 5-folds, with accompanying  
401 confidence intervals and standard deviations. We compared  
402 performance of several state-of-the-art time dependent models  
403 (Temporal Convolutional Network (TCN), Sequence of Gener-  
404 alized Linear Models (SGLM) with Elastic net regularization)  
405 and the baseline model (Random Forest).

406 Sequences of Bi-LSTMs outperformed the other models  
407 (Fig. 3a). Sequences of Bi-LSTMs, Sequences of TCNs, and  
408 SGLM with Elastic net were all able to leverage long term  
409 temporal dependencies to improve predictions. The perfor-  
410 mance of these three models increased approximately mono-  
411 tonically with time. The other two models with short-term  
412 time dependencies (independent Bi-LSTMs and TCNs) and  
413 Random Forest achieved better performance in two time-  
414 ranges: approximately 24-42 h and 66-78 h after cardiac arrest.  
415 The look-back strategy implemented in the Bi-LSTMs model  
416 was able to effectively leverage historical predictions and  
417 provide a trajectory of outcome risk for individual patients.

418 Performance of the various models was similar early after  
419 cardiac arrest (before 18 h), while performance of the Bi-  
420 LSTM model moderately increased to 0.87 (95% confidence  
421 interval, 95% CI: 0.84-0.89, standard deviation, std: 0.03) at 42  
422 h and reached its maximum value of 0.88 (95% CI: 0.85-0.91,  
423 std: 0.03) at 66 h. The AUC improvement of the sequence of  
424 Bi-LSTM model at 66h compared to Bi-LSTM, sequences of  
425 TCNs, TCN, SGLM with Elastic net, and Random Forest was  
426 0.03\*, 0.02, 0.08\*, 0.02, and 0.07\*; where \* indicates passing  
427 a test of statistical significance ( $p < 0.05$ ,  $t$ -test).

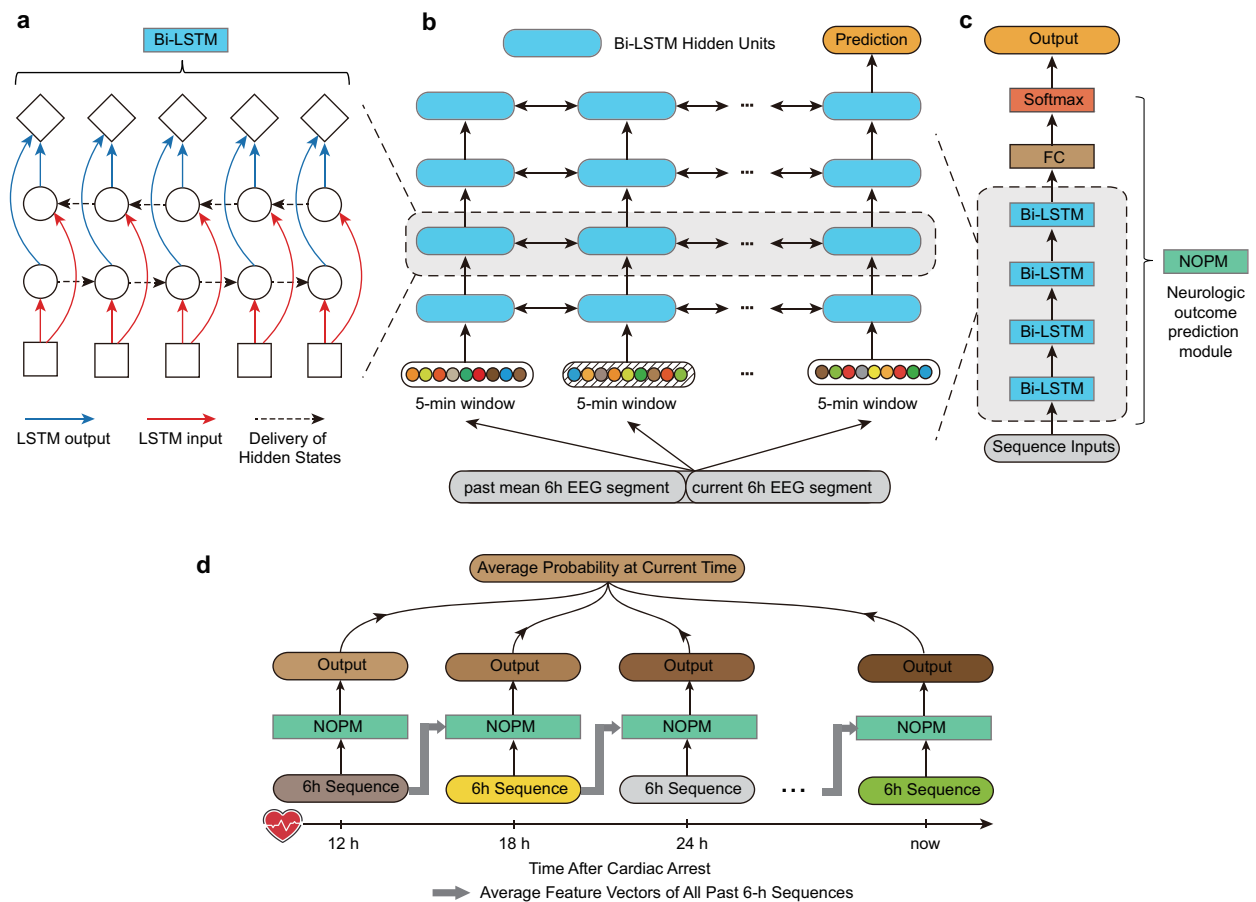


**Fig. 2.** Model architecture of a sequence of Bi-LSTMs. a, Dependencies between time steps in the EEG sequences were learned by a Bidirectional LSTM. b, A time-dependent deep learning model was developed that takes as input 6-h sequences of past mean and current EEG feature values. The outputs of hidden states in the last Bi-LSTM block were used for prediction. In cases of intermittent missing data (periods when EEG monitoring was interrupted), missing epochs (shaded blocks) were interpolated to values in the nearest available epochs. c, The best network architecture of individual 6-h time blocks consists of four Bi-LSTM layers, three dropout layers, one fully connected layer, and one softmax layer. The neural network was called a neurologic outcome prediction module (NOPM). d, To leverage the output probabilities of Bi-LSTMs at different time blocks and obtain more stable and robust predictions, we averaged the output probabilities of a sequence of Bi-LSTMs until now as the final prediction probabilities.

428 Although predictions made by the model are probabilities, 429 it is customary to compare these to thresholds and report 430 the statistical performance of the resulting binary predictions. 431 Doing this, performance of the model at 66 h was as follows. 432 For predicting poor outcomes, at specificity thresholds of 99%, 433 95%, and 90%, the models sensitivity was 32%, 55%, and 434 62%, respectively; whereas at sensitivity thresholds of 99%, 435 95%, and 90%, specificity was 23%, 47%, and 62%. For 436 predicting good outcomes, at specificity thresholds of 99%, 437 95%, and 90%, sensitivity was 17%, 47%, and 62%; whereas 438 at sensitivity thresholds of 99%, 95%, and 90%, specificity 439 was 19%, 48%, and 70%.

440 The improvement of all models with increasing time provides 441 evidence that leveraging long-term time dynamics of 442 EEG signals provides improved ability to predict neurologic 443 outcome. Sequences of Bi-LSTMs, Sequences of TCNs, and 444 SGLM with Elastic net had consistent improvement in performance 445 with more observations (from mean AUC of 0.78, 0.77, and 0.75 446 at 12 h to mean AUC of 0.88, 0.86, and 0.87 447 at 66 h, respectively). The improvement of the three models 448 was statistically significant ( $p < 0.01$ ,  $t$ -test).

449 It should be noted that the numbers of patients with available

EEG data varied over time (Fig. 3b). The numbers of patients 450 increased initially and decreased later, reaching a maximal 451 value of 826 during the time period 24–30 h. The ROC curves 452 at different times are shown in Fig. 3c. 453

### B. Calibration Risk

454 Model calibration was evaluated by comparing the predicted 455 probability of a poor outcome with the proportion of patients 456 who had a poor outcome. We compared calibration curves at 457 different time intervals and calculated calibration errors to 458 quantify performance (Fig. 3d). Calibration error was defined 459 as the absolute deviation from the diagonal line, which represents 460 perfect calibration (lack of systematic errors of over- 461 or under-prediction). Model calibration improved from 12 h 462 to 60 h and deteriorated after 60 h. Calibration error at 66 h 463 was 0.04. Our proposed model was well calibrated, with good 464 agreement between the observed proportions of poor outcomes 465 and predicted probabilities of poor outcomes. 466

### C. Subgroup Analysis

467 Having investigated overall performance on the whole cohort, 468 we next investigated prediction performance in individual 469

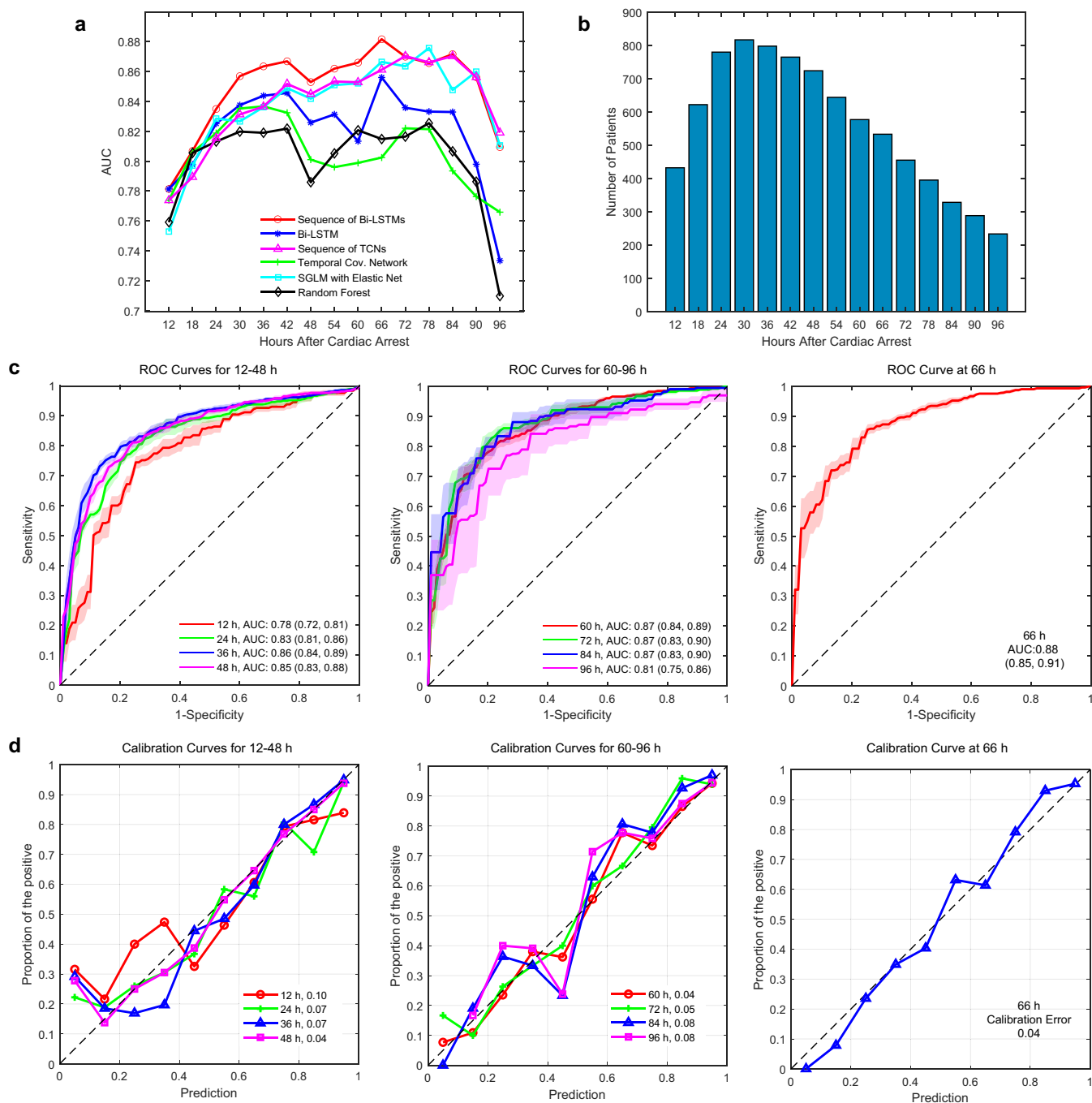


**Fig. 3.** Model performance of different models in outcome prediction. **a**, Mean AUC values of different models within each 6-hour time interval. Sequences of Bi-LSTMs (red line) performed best, exhibiting consistent improvement in performance with more observations (from mean AUC of 0.7814 at 12 h to mean AUC of 0.8815 at 66 h). **b**, Numbers of patients with EEG available with respect to time after cardiac arrest. **c**, Mean ROC curves at different time intervals (12-48 h, 60-96 h, and 66 h). Shaded areas indicate the standard errors in 5-fold cross validation. **d**, Calibration curves at different time intervals (12-48 h, 60-96 h, and 66 h). The numbers are calibration errors (deviations from the diagonals).

470 patients and CPC groups. Fig. 4a makes evident qualitatively  
 471 (in a colormap) that the sequence of Bi-LSTM prediction  
 472 probabilities over time in all individual patients. For some  
 473 patients identified initially as having a low predicted proba-  
 474 bility of a good outcome, the predicted probability of a good  
 475 outcome increases progressively as additional observations  
 476 come in over time, and in general, predicted probabilities are  
 477 more accurate at later time points. These results support our  
 478 starting hypothesis, that leveraging long term EEG dynamics

can improve prediction performance of neurologic prognosti- 479  
 cation models. While model predictions generally agree well 480  
 with observed outcomes, in keeping with the probabilistic 481  
 framework, the models predictions are not infallible. Poor 482  
 outcomes occasionally occur despite confident predictions of 483  
 a good outcome, and vice versa (Fig. 4a). 484

Next, we grouped outcome prediction probabilities by CPC 485  
 scores (Fig. 4b). The mean predicted probability of poor 486  
 outcome within each CPC group was consistent with the 487

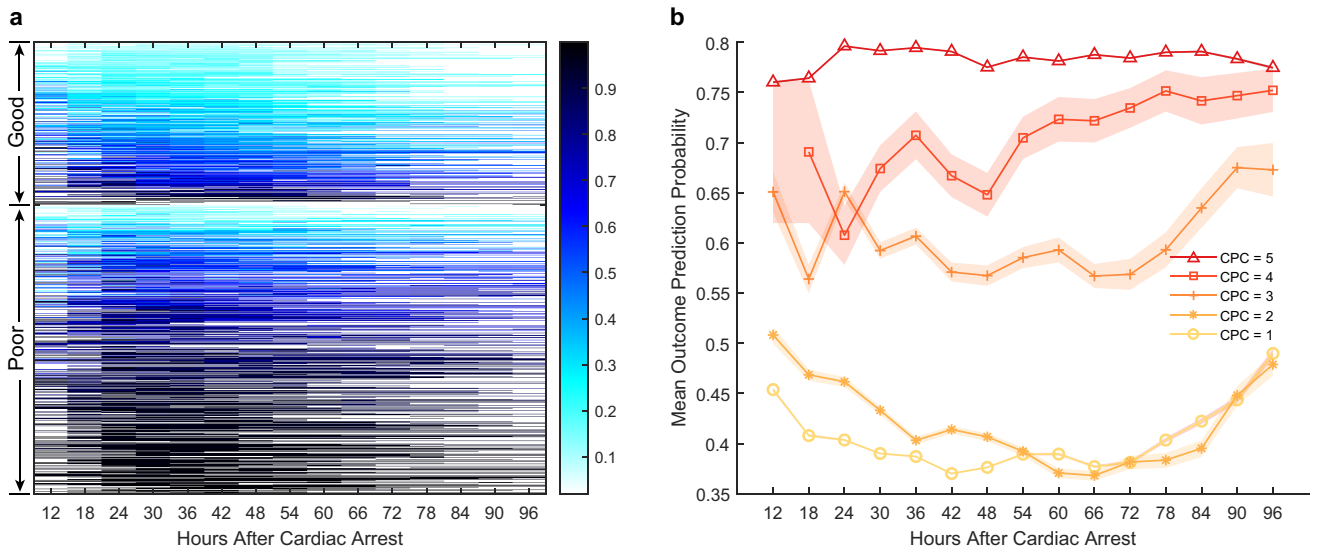


**Fig. 4.** Prediction probabilities of poor outcome over time for individual patients and individual CPC groups. a, Individual prediction probabilities of poor outcome can change over time. Each row shows the output probabilities from our model for one patient over consecutive 6h blocks, the darker the color, the higher the predicted probability of poor outcome. Patients in each outcome group are sorted based on the mean prediction probabilities. Generally, the group with poor outcomes has substantially higher predicted probabilities of poor outcomes. b, Predicted probabilities over time, grouped by final CPC scores. A CPC score of 1 denotes good recovery while CPC score of 5 denotes death. The overall mean predicted probabilities were consistent with the expected order of CPC scores.

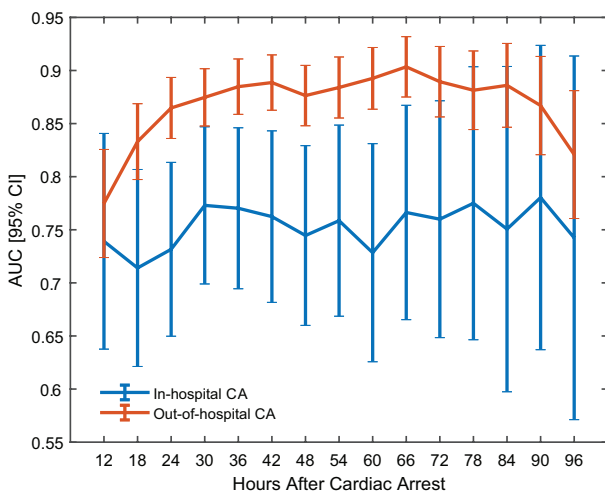


**Fig. 5.** Model performance of out-of-hospital cardiac arrest and in-hospital cardiac arrest over time.

488 ordinal ordering of CPC scores. The CPC 5 group had the  
 489 highest mean prediction probabilities, while the CPC 1 group  
 490 had the lowest mean prediction probabilities of poor outcomes.  
 491 The mean prediction probabilities of the CPC 1-5 groups were  
 492 0.41, 0.42, 0.61, 0.71, and 0.78, respectively. There was a large  
 493 probability gap between the group with good outcomes (CPC  
 494 1-2) and the group with poor outcomes (CPC 3-5).

495 For subgroup analysis, we evaluated the model performance  
 496 for patients with out-of-hospital cardiac arrest and in-hospital  
 497 cardiac arrest, respectively, after five-fold cross validation (Fig.  
 498 5). Most patients in our dataset were patients with out-of-  
 499 hospital cardiac arrest: 761 patients (73%) had out-of-hospital  
 500 cardiac arrest, 203 (20%) in-hospital cardiac arrest, and 74  
 501 patients (7%) did not have that data available. Overall, the

performance of the out-of-hospital cohort were better than  
 those of the in-hospital cohort. The performance of the in-  
 hospital cohort were similar over the time intervals after CA  
 while those of out-hospital cohort increased moderately over  
 time and reached a best AUC of 90% [88%, 93%] at 66 hours  
 after CA.

We last investigated whether model performance varied  
 across patients cared for at different institutions. Model per-  
 formance varied between institutions (Table II). Notably, out-  
 comes were most predictable early (0-24 hours) on within the  
 two Dutch hospitals (UTW, RIJ), reaching an AUC of 89% by  
 24 hours, whereas outcome predictability reached only AUC  
 of 66% within the Belgian hospital (ULB).

#### D. Visualization

The modeling framework was inspired by actual clinical  
 decision making, which considers current EEG information  
 in context with historical information to predict neurologic  
 outcome. Model performance on five typical cases is illustrated  
 in Fig. 6, each with a different CPC score. The mean spec-  
 trograms and corresponding EEG snapshots are shown. From  
 the figure, we see that the prediction probabilities follow the  
 rank order of neurologic outcomes (CPC scores).

The first two patients with good outcomes (CPC 1 and 2)  
 had continuous EEG patterns with normal amplitudes during  
 recovery. Early improvements to continuous EEG patterns  
 usually indicate a good outcome. Their spectrograms demon-  
 strate improving power in low frequency bands. Prediction  
 probabilities of poor outcomes were consistently low for both  
 patients over time. The patient with CPC 3 had isoelectric  
 EEG early at 12-24 h after cardiac arrest. Early isoelectric  
 EEG had an intermediate probability of a poor outcome.  
 However, prolongation of the isoelectric pattern increased the



**TABLE II**  
MODEL PERFORMANCE FOR INDIVIDUAL INSTITUTIONS (AUC, 95% CONFIDENCE INTERVALS)

Time Interval	12 h	18 h	24 h	30 h	36 h
BIDMC	0.68 [0.50,0.85]	0.74 [0.61,0.87]	0.80 [0.69,0.90]	0.81 [0.72,0.91]	0.83 [0.75,0.92]
BWH	0.82 [0.69,0.95]	0.75 [0.63,0.86]	0.73 [0.63,0.82]	0.76 [0.67,0.85]	0.71 [0.62,0.80]
MGH	0.77 [0.59,0.94]	0.80 [0.70,0.91]	0.88 [0.81,0.95]	0.90 [0.84,0.96]	0.88 [0.81,0.94]
ULB	0.62 [0.48,0.76]	0.64 [0.52,0.76]	0.66 [0.56,0.76]	0.71 [0.61,0.80]	0.75 [0.66,0.85]
UTW+RS	0.82 [0.76,0.87]	0.85 [0.81,0.90]	0.89 [0.85,0.92]	0.89 [0.86,0.93]	0.90 [0.87,0.94]
YNH	0.59 [0.41,0.77]	0.81 [0.70,0.92]	0.87 [0.78,0.95]	0.90 [0.83,0.97]	0.93 [0.87,0.98]
Time Interval	42 h	48 h	54 h	60 h	66 h
BIDMC	0.82 [0.73,0.92]	0.82 [0.72,0.91]	0.85 [0.76,0.94]	0.85 [0.76,0.94]	0.85 [0.74,0.95]
BWH	0.74 [0.65,0.83]	0.73 [0.64,0.83]	0.76 [0.67,0.85]	0.73 [0.64,0.83]	0.73 [0.63,0.83]
MGH	0.88 [0.82,0.94]	0.84 [0.77,0.91]	0.87 [0.80,0.93]	0.89 [0.83,0.95]	0.93 [0.88,0.98]
ULB	0.77 [0.67,0.87]	0.69 [0.56,0.81]	0.63 [0.46,0.80]	0.61 [0.42,0.80]	0.66 [0.47,0.84]
UTW+RS	0.91 [0.87,0.94]	0.91 [0.87,0.94]	0.91 [0.87,0.95]	0.91 [0.87,0.95]	0.91 [0.87,0.95]
YNH	0.92 [0.86,0.98]	0.91 [0.85,0.97]	0.91 [0.85,0.98]	0.94 [0.88,0.99]	0.95 [0.89,1.00]
Time Interval	72 h	78 h	84 h	90 h	96 h
BIDMC	0.86 [0.76,0.96]	0.85 [0.73,0.96]	0.89 [0.78,1.00]	0.88 [0.76,1.00]	0.86 [0.71,1.00]
BWH	0.71 [0.59,0.83]	0.77 [0.66,0.89]	0.81 [0.70,0.92]	0.79 [0.67,0.92]	0.70 [0.54,0.86]
MGH	0.90 [0.83,0.96]	0.92 [0.86,0.98]	0.92 [0.86,0.99]	0.93 [0.86,1.00]	0.92 [0.84,1.00]
ULB	0.63 [0.42,0.83]	0.60 [0.40,0.80]	0.56 [0.34,0.78]	0.54 [0.32,0.76]	0.46 [0.22,0.70]
UTW+RS	0.91 [0.86,0.95]	0.91 [0.86,0.96]	0.89 [0.83,0.95]	0.88 [0.81,0.95]	0.85 [0.76,0.94]
YNH	0.94 [0.88,1.00]	0.90 [0.80,0.99]	0.95 [0.87,1.00]	0.94 [0.87,1.00]	0.94 [0.85,1.00]

BIDMC: Beth Israel Deaconess Medical Center, BWH: Brigham and Womens Hospital, MGH: Massachusetts General Hospital, ULB: Erasmus Hospital, Universit Libre de Bruxelles, UTW: Medisch Spectrum Twente, and Rijnstate Hospital, University of Twente, YNH: Yale New Haven Hospital.

534 probability of a poor outcome (from 32.77% at 12 h to  
535 48.03% at 24 h). Later the EEG evolved to have more and  
536 more epileptiform discharges (generalized periodic discharges)  
537 and the patient experienced seizures. With continuation of  
538 unfavorable EEG patterns throughout the first 72 hours, the  
539 prediction probability of a poor outcome from our model  
540 reached 81.56% by 72 hours. The patient with CPC 4 had  
541 a high burst-suppression ratio with epileptiform discharges  
542 lasting for more than 12 hours. The evolution of the EEG to  
543 continuous patterns occurred late (e.g., after 48 h). Therefore,  
544 the output probabilities of a poor outcome were relatively high  
545 over time. The EEG of the patient with the worst outcome  
546 (CPC 5) showed persistent voltage suppression (last row of  
547 Fig. 6). This patient had a high burst-suppression ratio with  
548 highly epileptiform bursts. The prediction probabilities for  
549 this patient were high throughout the entire course of EEG  
550 monitoring (over 95%).

#### 551 IV. DISCUSSION

552 Our results demonstrate that a deep learning model that  
553 leverages EEG dynamics can provide accurate neurologic  
554 outcome predictions post-cardiac arrest that become more  
555 accurate as time passes. Our time-sensitive models accuracy  
556 continued to increase as additional EEG data was included,  
557 reaching maximum predictive accuracy at 66 hours (AUC  
558 0.88). The model was well calibrated, with observed pro-  
559 portions of poor outcomes closely matching predicted prob-  
560 abilities. Further, outcome probabilities mapped closely onto  
561 observed outcome categories, following the rank order of  
562 CPC scores. These individual-level outcome probabilities of  
563 the model are suitable for risk stratification for neurologic  
564 outcome prediction after cardiac arrest. Additional relevant  
565 features of this study is its size, with more than 1,000  
566 prospectively collected cases, and the inclusion of patients  
567 from seven different hospitals from three countries (United

States, Netherlands, and Belgium). 568

This work builds on several prior studies using quantita- 569  
570 tive analysis of EEG data to predict neurologic outcome in  
571 postanoxic coma. Most prior studies have used time-insensitive  
572 models, which make predictions based on EEG data available  
573 from specific epochs, e.g. 0-12 hours, 12-24 hours. [20], [21],  
574 [29], [31], [32] Partial exceptions are the Cerebral Recovery  
575 Index (CRI) models, of which there have been three versions  
576 [20], [21], [32], all from studies performed in the Netherlands.  
577 The first utilized 109 patients from 1 hospital; the second,  
578 238 patients from two hospitals (UTW, RS); the third, from  
579 551 patients from the same two hospitals (a subset of the I-  
580 CARE cohort in the present study). Unlike most prior work,  
581 the three CRI studies investigate prediction performance over  
582 time. Maximal AUC was achieved in the original CRI paper  
583 at 18 h (0.94) using a hand-crafted parametric model with 5  
584 QEEG features [20]; at 12 h (0.92) in the second CRI using  
585 random forest model employing 9 QEEG features [21]; and  
586 at 12 h (0.94) in the third CRI employing 44 features in a  
587 random forest model, supplemented with a feature selection  
588 procedure (LASSO regression) [32]. In contrast to the present  
589 work, none of the three CRI models attempted to leverage  
590 temporal trends to improve prediction performance over time.

In more recent work [29], the CRI authors utilized data 591  
592 from 895 patients from 5 Dutch hospitals, to train a convo-  
593 lutional neural network (CNN) to predict neurologic outcome  
594 at two time points (12 and 24 hours). The authors also tried  
595 concatenating EEG inputs from 12 and 24 hours. Maximal  
596 performance on the validation set was achieved at 12 hours  
597 (AUC 0.92); though performance for the model that combined  
598 information from 12 and 24 hour was essentially the same  
599 (AUC 0.91). However, the authors did not explicitly investigate  
600 the prognostic value of EEG trends and did not attempt to  
601 leverage the full temporal evolution of the EEG; it is possible  
602 that even better performance could have been achieved by

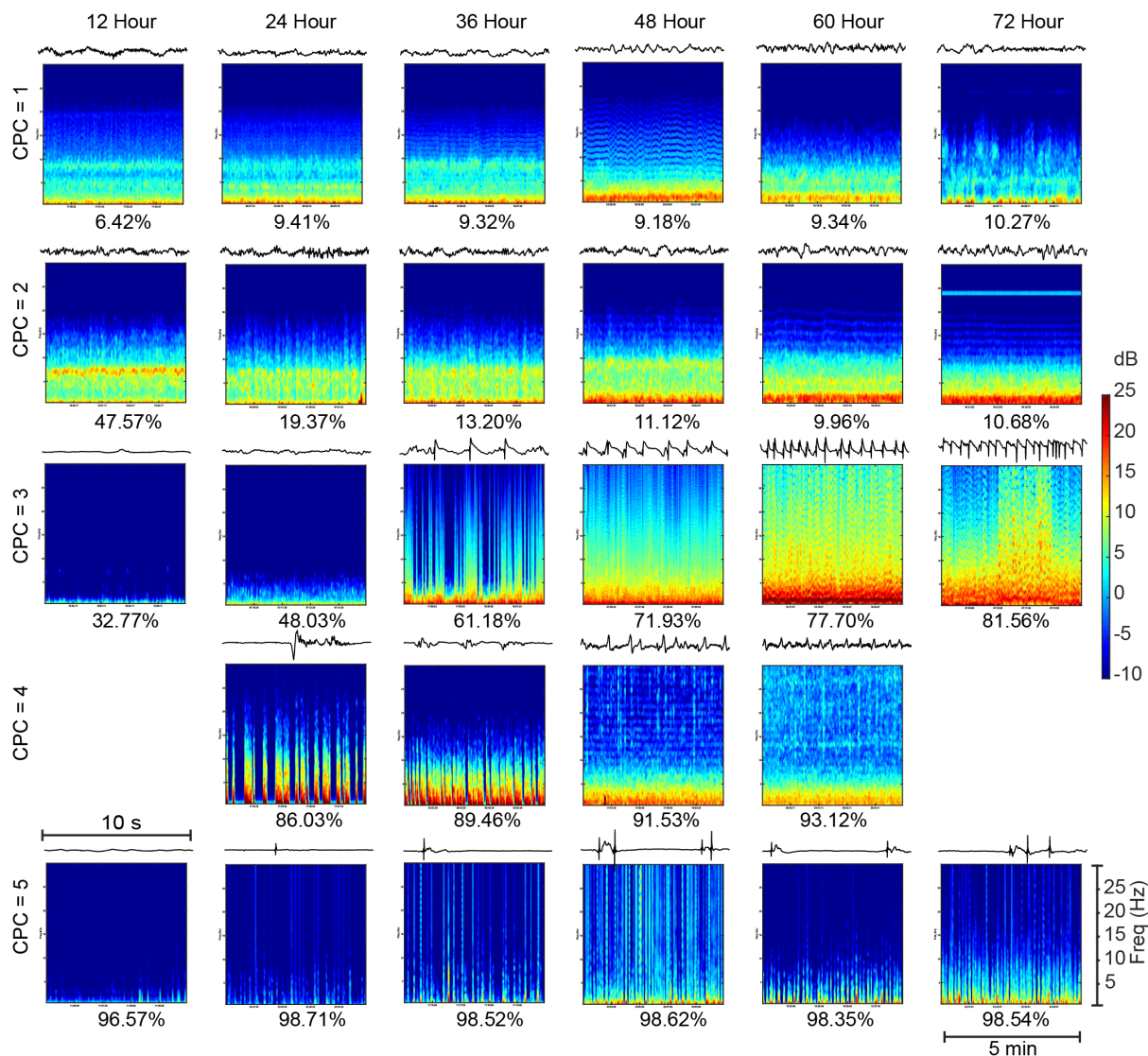


Fig. 6. Model performance on sample patients. Each row illustrates the mean multi-taper spectrogram and EEG waveforms in multiple time blocks. At the bottom of each spectrogram, prediction probabilities of the model for the corresponding EEG segments are shown. The time length of EEG snapshots was 10 s while the spectrograms spanning a 5-min time window are shown. Generally, continuous EEGs had low prediction probabilities of poor outcomes while burst-suppression patterns and epileptiform discharges produced high prediction probabilities of poor outcomes.

603 leveraging temporal trends. One recent study that did explicitly  
 604 attempt to construct a time-sensitive model utilized data from  
 605 438 patients from four US hospitals, to train a sequence  
 606 of Generalized Linear Models (SGLM) with 52 QEEG fea-  
 607 tures as input (with elastic net feature selection). [31] The  
 608 time-sensitive SGLM model demonstrated monotonically im-  
 609 proving prediction over time, by making use of a memory  
 610 bank of progressively more EEG feature vectors from prior  
 611 epochs, and achieved a maximal AUC of 0.83 by 72 hours.  
 612 The predictive performance of individual features recorded  
 613 at different time points changed over time, indicating that  
 614 the discriminative power of EEG data is both time-dependent  
 615 and feature-specific. On the same data set, the time-sensitive  
 616 model performed better than a random forest model based on  
 617 the second CRI model (AUC 0.83 vs. 0.74, respectively). In  
 618 addition to measuring performance by AUC, the SGLM paper  
 619 also introduced the concept of model calibration (how well the

620 predicted probability of good or poor outcome agrees with the  
 621 observed frequency of outcomes) as a key indicator of model  
 622 performance, arguing that such probabilistic information is  
 623 more relevant to clinical decision making than simple binary  
 624 predictions (with accompanying measures of sensitivity and  
 625 specificity). The SGLM model was shown to have excellent  
 626 calibration across the initial 72 hours of EEG monitoring,  
 627 superior to several time-insensitive approaches [31].

628 In the current study, we utilized data from 1038 patients  
 629 from 7 hospitals in 3 countries, the largest and most diverse  
 630 dataset assembled to date to develop machine learning models  
 631 to predict neurologic outcome in postanoxic coma. We directly  
 632 compared a wide variety machine learning models on the  
 633 same data, including several of the prior best performing  
 634 models (e.g. random forest and SGLM), in addition to several  
 635 new model types. Best performance was achieved by a time-  
 636 sensitive model Bi-LSTM model, which showed monotonically

637 cally increasing performance up to 66 hours. The Bi-LSTM  
638 model performed slightly better than the time-sensitive elastic  
639 net model (AUC 0.88 vs. 0.86, respectively). In addition, the  
640 Bi-LSTM model was superior to other state-of-the-art machine  
641 learning models (sequence of TCN and Random Forests).

642 It is important to note that model prediction statistics (e.g.  
643 AUC values) cannot be directly compared across prior studies.  
644 Important differences between studies include: 1) The current  
645 data set is larger; 2) the current data set is more heterogeneous,  
646 coming from seven hospitals and three different countries.  
647 Indeed, our data suggest that predictability of neurologic  
648 outcome likely varies substantially between centers, thus  
649 between-center heterogeneity may be consequential. Possible  
650 reasons for differential predictability include differences in  
651 patient characteristics, care practices, and decision-making  
652 regarding withdrawal of care. Careful future study of this issue  
653 is warranted. 3) Model training and validation strategies differ  
654 across studies. 4) Model evaluation practices differed across  
655 studies. An important feature of the original elastic net study  
656 and the current Bi-LSTM model lacking in prior studies is the  
657 emphasis on model calibration. Calibration provides a measure  
658 of a models ability to provide clinically relevant probabilistic  
659 estimates of risk, which can be done at the individual patient-  
660 level and across all predicted probabilities, without artificially  
661 imposing pre-specified binary thresholds.

662 Our study has several important limitations. 1), As seen in  
663 Fig. 4a, prediction is not perfect; there exist cases where model  
664 fails to make the correct prediction consistently throughout  
665 EEG monitoring. It is possible that calibrating the general-  
666 purpose model developed herein to characteristics of individ-  
667 ual patients could further improve prediction performance. 2),  
668 Our model utilized only EEG information. Baseline patient and  
669 treatment characteristics are also associated with outcome after  
670 cardiac arrest, e.g., location of arrest, first recorded rhythm,  
671 time from 911 call to sustained restoration of circulation,  
672 and method of induced hypothermia/targeted temperature man-  
673 agement. Incorporating a wider array of information might  
674 further improve outcome predictability. However, not all of  
675 these clinical variables were available due to different data  
676 collection protocols in different centers. 3), In the present  
677 study we focused on nine clinically interpretable EEG features.  
678 We did not include all features known to be associated with  
679 poor outcomes. For example, as mentioned above, we did not  
680 quantify similarity between bursts in burst suppression. Sim-  
681 ilarly, although we included information about the frequency  
682 of epileptiform discharges and background amplitude, we did  
683 not explicitly account for the periodicity of discharges, nor  
684 did we explicitly construct a feature which looked for the  
685 conjunction of generalized periodic discharges and a flat or  
686 low voltage background, another pattern strongly associated  
687 with poor outcomes. [9], [11] It is possible that including  
688 information about such features more explicitly would further  
689 improve model performance. 4), It is possible that additional  
690 ‘data driven’ features, beyond those described in the literature,  
691 might further improve model performance. Some prior EEG  
692 studies (outside the field of cardiac arrest prognostication)  
693 have developed hybrid deep neural networks which combine  
694 convolutional neural networks (CNN) and recurrent neural

695 networks (RNN) for EEG time series, where EEG features  
696 are automatically learned from raw waveforms with CNN and  
697 time dependencies between are modeled with RNN models.  
698 Such hybrid network architectures (CNN-RNN) have been  
699 validated in some time series applications [41], [42], and this  
700 is a promising future direction for our work. 5), Treating  
701 physicians were not blinded to EEG results in the present  
702 study, and thus may have used these results for decision  
703 making regarding continuation of life-sustaining treatment.  
704 Therefore, we could not exclude the risk of self-fulfilling  
705 prophecies introducing model prediction bias. 6), The EEG  
706 data were collected at different clinical sites, not as part  
707 of a single unified study. Therefore, we have evaluated the  
708 model performance on the data from independent studies.  
709 But the generalization of the proposed model should be  
710 further evaluated on more heterogeneous patient cohorts from  
711 different clinical centers. 7), The proportion of patients with  
712 good outcome was comparable to other studies in the literature  
713 [29], [31].

714 Use of sedatives is common in comatose cardiac arrest  
715 patients, however, the effect of sedatives on neurological  
716 outcomes have not been quantified, e.g., whether propofol is  
717 beneficial or harmful in patients with cell and organ injury  
718 after resuscitation from cardiac arrest is unknown. [43] Use  
719 of sedatives might have affected the EEG signals used in  
720 our prediction models and might impact the generalizability  
721 of the study results. [44] Recent studies suggest that the  
722 influence of sedatives on EEG patterns does not significantly  
723 affect neurological prognostication performance. [37], [45],  
724 [46] Nevertheless, usage and dosing of sedative drugs varies  
725 across sites, and the effects of propofol and other sedatives  
726 in individual critically ill patients varies, thus further inves-  
727 tigation of individual-level effects and effect variation across  
728 medical centers remains an important topic for investigation.

729 In the past few decades, neurologic prognostication after  
730 cardiac arrest has progressed towards a multimodal paradigm  
731 based on integrating information from the clinical examination  
732 (e.g. the pupillary light and corneal reflex) with information  
733 from other modalities, e.g. somatosensory evoked potential,  
734 brain imaging [47]–[50]. Given that different modalities have  
735 strengths and weaknesses, multimodality assessments may  
736 provide more reliable neurologic prognostication by combin-  
737 ing clinical evidence from multiple complementary informa-  
738 tion sources [7], [51], [52]. Future work on developing more  
739 robust multimodal outcome prediction models should focus on  
740 well-designed deep learning models that integrate rich, large-  
741 scale healthcare data [24], [53], [54] from various institutions  
742 to encompass wider practice variations and a broader range of  
743 patient phenotypes to improve model performance.

## 744 V. CONCLUSION

745 In conclusion, we developed a time-sensitive deep learning  
746 model for neurological outcome prediction in coma patients  
747 after CA with sequences of Bi-LSTMs, which can learn  
748 the long-term EEG dynamics during the progressive course  
749 of coma recovery. Model performance was evaluated on a  
750 large, multicenter, international cohort, and the model showed

751 excellent agreement between its probabilistic predictions and  
752 the observed rate of good and poor neurologic outcomes. Our  
753 results demonstrate that time-sensitive deep neural networks  
754 can extract valuable information from the EEG in patients with  
755 coma following cardiac arrest, to provide accurate predictions  
756 about the potential recovery of neurologic function.

## 757 REFERENCES

- 758 [1] E. J. Benjamin, P. Muntner, A. Alonso, M. S. Bittencourt, C. W.  
759 Callaway, A. P. Carson, A. M. Chamberlain, A. R. Chang, S. Cheng,  
760 S. R. Das *et al.*, "Heart disease and stroke statistics 2019 update: a report  
761 from the american heart association," *Circulation*, vol. 139, no. 10, pp.  
762 e56–e528, 2019.
- 763 [2] N. Nielsen, J. Wetterslev, T. Cronberg, D. Erlinge, Y. Gasche, C. Has-  
764 sager, J. Horn, J. Hovdenes, J. Kjaergaard, M. Kuiper *et al.*, "Targeted  
765 temperature management at 33 c versus 36 c after cardiac arrest," *New*  
766 *England Journal of Medicine*, vol. 369, no. 23, pp. 2197–2206, 2013.
- 767 [3] C. W. Callaway, M. W. Donnino, E. L. Fink, R. G. Geocadin, E. Golan,  
768 K. B. Kern, M. Leary, W. J. Meurer, M. A. Peberdy, T. M. Thompson  
769 *et al.*, "Part 8: post-cardiac arrest care: 2015 american heart association  
770 guidelines update for cardiopulmonary resuscitation and emergency  
771 cardiovascular care," *Circulation*, vol. 132, no. 18\_suppl.2, pp. S465–  
772 S482, 2015.
- 773 [4] C. Sandroni, A. Cariou, F. Cavallaro, T. Cronberg, H. Friberg, C. Hoede-  
774 maekers, J. Horn, J. P. Nolan, A. O. Rossetti, and J. Soar, "Prognostica-  
775 tion in comatose survivors of cardiac arrest: an advisory statement from  
776 the european resuscitation council and the european society of intensive  
777 care medicine," *Intensive Care Medicine*, vol. 40, no. 12, pp. 1816–1831,  
778 2014.
- 779 [5] G. B. Young, "Neurologic prognosis after cardiac arrest," *New England*  
780 *Journal of Medicine*, vol. 361, no. 6, pp. 605–611, 2009.
- 781 [6] D. K. Hahn, R. G. Geocadin, and D. M. Greer, "Quality of evidence in  
782 studies evaluating neuroimaging for neurologic prognostication in adult  
783 patients resuscitated from cardiac arrest," *Resuscitation*, vol. 85, no. 2,  
784 pp. 165–172, 2014.
- 785 [7] A. O. Rossetti, A. A. Rabinstein, and M. Oddo, "Neurological prognos-  
786 tication of outcome in patients in coma after cardiac arrest," *The Lancet*  
787 *Neurology*, vol. 15, no. 6, pp. 597–609, 2016.
- 788 [8] E. F. Wijdicks, A. Hijdra, G. Young, C. Bassetti, and S. Wiebe,  
789 "Practice parameter: prediction of outcome in comatose survivors after  
790 cardiopulmonary resuscitation (an evidence-based review): report of the  
791 quality standards subcommittee of the american academy of neurology,"  
792 *Neurology*, vol. 67, no. 2, pp. 203–210, 2006.
- 793 [9] B. J. Ruijter, M. C. Tjepkema-Cloostermans, S. C. Tromp, W. M. van den  
794 Bergh, N. A. Foudraïne, F. H. Kornips, G. Drost, E. Scholten, F. H.  
795 Bosch, A. Beishuizen *et al.*, "Early electroencephalography for outcome  
796 prediction of postanoxic coma: a prospective cohort study," *Annals of*  
797 *Neurology*, vol. 86, no. 2, pp. 203–214, 2019.
- 798 [10] M. M. Admiraal, A.-F. van Rootselaar, J. Hofmeijer, C. W. Hoedemaek-  
799 ers, C. R. van Kaam, H. M. Keijzer, M. J. van Putten, M. J. Schultz, and  
800 J. Horn, "Electroencephalographic reactivity as predictor of neurological  
801 outcome in postanoxic coma: a multicenter prospective cohort study,"  
802 *Annals of Neurology*, vol. 86, no. 1, pp. 17–27, 2019.
- 803 [11] E. Westhall, A. O. Rossetti, A.-F. van Rootselaar, T. W. Kjaer, J. Horn,  
804 S. Ullén, H. Friberg, N. Nielsen, I. Rosén, A. Åneman *et al.*, "Stan-  
805 dardized EEG interpretation accurately predicts prognosis after cardiac  
806 arrest," *Neurology*, vol. 86, no. 16, pp. 1482–1490, 2016.
- 807 [12] J. Hofmeijer, M. C. Tjepkema-Cloostermans, and M. J. van Putten,  
808 "Burst-suppression with identical bursts: a distinct EEG pattern with  
809 poor outcome in postanoxic coma," *Clinical Neurophysiology*, vol. 125,  
810 no. 5, pp. 947–954, 2014.
- 811 [13] M. C. Tjepkema-Cloostermans, J. Hofmeijer, R. J. Trof, M. J. Blans,  
812 A. Beishuizen, and M. J. van Putten, "Electroencephalogram predicts  
813 outcome in patients with postanoxic coma during mild therapeutic  
814 hypothermia," *Critical Care Medicine*, vol. 43, no. 1, pp. 159–167, 2015.
- 815 [14] A. Sivaraju, E. J. Gilmore, C. R. Wira, A. Stevens, N. Rampal, J. J.  
816 Moeller, D. M. Greer, L. J. Hirsch, and N. Gaspard, "Prognostication  
817 of post-cardiac arrest coma: early clinical and electroencephalographic  
818 predictors of outcome," *Intensive Care Medicine*, vol. 41, no. 7, pp.  
819 1264–1272, 2015.
- 820 [15] S. Tsetsou, J. Novy, M. Oddo, and A. O. Rossetti, "EEG reactivity to  
821 pain in comatose patients: importance of the stimulus type," *Resuscita-*  
822 *tion*, vol. 97, pp. 34–37, 2015.
- [16] E. Amorim, J. C. Rittenberger, J. J. Zheng, M. B. Westover, M. E.  
823 Baldwin, C. W. Callaway, A. Popescu *et al.*, "Continuous EEG moni-  
824 toring enhances multimodal outcome prediction in hypoxic-ischemic  
825 brain injury," *Resuscitation*, vol. 109, pp. 121–126, 2016.
- [17] J. Jing, A. Herlopian, I. Karakis, M. Ng, J. J. Halford, A. Lam,  
827 D. Maus, F. Chan, M. Dolatshahi, C. F. Muniz *et al.*, "Interrater  
828 reliability of experts in identifying interictal epileptiform discharges in  
829 electroencephalograms," *JAMA Neurology*, vol. 77, no. 1, pp. 49–57,  
830 2020.
- [18] M. C. Hermans, M. B. Westover, M. J. van Putten, L. J. Hirsch, and  
831 N. Gaspard, "Quantification of EEG reactivity in comatose patients,"  
832 *Clinical Neurophysiology*, vol. 127, no. 1, pp. 571–580, 2016.
- [19] N. Gaspard, L. J. Hirsch, S. M. LaRoche, C. D. Hahn, M. B. Westover,  
835 and C. C. E. M. R. Consortium, "Interrater agreement for critical care  
836 EEG terminology," *Epilepsia*, vol. 55, no. 9, pp. 1366–1373, 2014.
- [20] M. C. Tjepkema-Cloostermans, F. B. van Meulen, G. Meinsma, and  
838 M. J. van Putten, "A cerebral recovery index (CRI) for early prognosis  
839 in patients after cardiac arrest," *Critical Care*, vol. 17, no. 5, pp. 1–11,  
840 2013.
- [21] M. C. Tjepkema-Cloostermans, J. Hofmeijer, A. Beishuizen, H. W. Hom,  
842 M. J. Blans, F. H. Bosch, and M. J. Van Putten, "Cerebral recovery index:  
843 reliable help for prediction of neurologic outcome after cardiac arrest,"  
844 *Critical Care Medicine*, vol. 45, no. 8, pp. e789–e797, 2017.
- [22] S. Lee, X. Zhao, K. A. Davis, A. A. Topjian, B. Litt, and N. S. Abend,  
846 "Quantitative EEG predicts outcomes in children after cardiac arrest,"  
847 *Neurology*, vol. 92, no. 20, pp. e2329–e2338, 2019.
- [23] J. Hofmeijer, T. M. Beernink, F. H. Bosch, A. Beishuizen, M. C.  
849 Tjepkema-Cloostermans, and M. J. van Putten, "Early EEG contributes  
850 to multimodal outcome prediction of postanoxic coma," *Neurology*,  
851 vol. 85, no. 2, pp. 137–143, 2015.
- [24] K.-H. Yu, A. L. Beam, and I. S. Kohane, "Artificial intelligence in  
853 healthcare," *Nature Biomedical Engineering*, vol. 2, no. 10, pp. 719–  
854 731, 2018.
- [25] A. Y. Hannun, P. Rajpurkar, M. Haghpanahi, G. H. Tison, C. Bourn,  
856 M. P. Turakhia, and A. Y. Ng, "Cardiologist-level arrhythmia detection  
857 and classification in ambulatory electrocardiograms using a deep neural  
858 network," *Nature Medicine*, vol. 25, no. 1, pp. 65–69, 2019.
- [26] R. Poplin, A. V. Varadarajan, K. Blumer, Y. Liu, M. V. McConnell,  
860 G. S. Corrado, L. Peng, and D. R. Webster, "Prediction of cardiovascular  
861 risk factors from retinal fundus photographs via deep learning," *Nature*  
862 *Biomedical Engineering*, vol. 2, no. 3, pp. 158–164, 2018.
- [27] J. Wiens, S. Saria, M. Sendak, M. Ghassemi, V. X. Liu, F. Doshi-Velez,  
864 K. Jung, K. Heller, D. Kale, M. Saeed *et al.*, "Do no harm: a roadmap for  
865 responsible machine learning for health care," *Nature Medicine*, vol. 25,  
866 no. 9, pp. 1337–1340, 2019.
- [28] W.-L. Zheng, H. Sun, O. Akeju, and M. B. Westover, "Adaptive sedation  
868 monitoring from EEG in ICU patients with online learning," *IEEE*  
869 *Transactions on Biomedical Engineering*, vol. 67, no. 6, pp. 1696–1706,  
870 2019.
- [29] M. C. Tjepkema-Cloostermans, C. da Silva Lourenço, B. J. Ruijter,  
872 S. C. Tromp, G. Drost, F. H. Kornips, A. Beishuizen, F. H. Bosch,  
873 J. Hofmeijer, and M. J. van Putten, "Outcome prediction in postanoxic  
874 coma with deep learning," *Critical Care Medicine*, vol. 47, no. 10, pp.  
875 1424–1432, 2019.
- [30] E. Amorim, M. Van der Stoel, S. B. Nagaraj, M. M. Ghassemi, J. Jing,  
877 U.-M. O'Reilly, B. M. Scirica, J. W. Lee, S. S. Cash, and M. B.  
878 Westover, "Quantitative EEG reactivity and machine learning for progn-  
879 nostication in hypoxic-ischemic brain injury," *Clinical Neurophysiology*,  
880 vol. 130, no. 10, pp. 1908–1916, 2019.
- [31] M. M. Ghassemi, E. Amorim, T. Alhanai, J. W. Lee, S. T. Herman,  
882 A. Sivaraju, N. Gaspard, L. J. Hirsch, B. M. Scirica, S. Biswal *et al.*,  
883 "Quantitative electroencephalogram trends predict recovery in hypoxic-  
884 ischemic encephalopathy," *Critical Care Medicine*, vol. 47, no. 10, pp.  
885 1416–1423, 2019.
- [32] S. B. Nagaraj, M. C. Tjepkema-Cloostermans, B. J. Ruijter, J. Hofmeijer,  
887 and M. J. van Putten, "The revised cerebral recovery index improves  
888 predictions of neurological outcome after cardiac arrest," *Clinical Neu-*  
889 *rophysiology*, vol. 129, no. 12, pp. 2557–2566, 2018.
- [33] C. M. Booth, R. H. Boone, G. Tomlinson, and A. S. Detsky, "Is this  
891 patient dead, vegetative, or severely neurologically impaired?: assessing  
892 outcome for comatose survivors of cardiac arrest," *JAMA*, vol. 291, no. 7,  
893 pp. 870–879, 2004.
- [34] F. S. Taccone, J. Horn, C. Storm, A. Cariou, C. Sandroni, H. Friberg,  
895 C. A. Hoedemaekers, and M. Oddo, "Death after awakening from post-  
896 anoxic coma: the best CPC project," *Critical Care*, vol. 23, no. 1, pp.  
897 1–8, 2019.

- 899 [35] M. B. Westover, M. M. Shafi, S. Ching, J. J. Chemali, P. L. Purdon, S. S.  
900 Cash, and E. N. Brown, "Real-time segmentation of burst suppression  
901 patterns in critical care EEG monitoring," *Journal of Neuroscience*  
902 *Methods*, vol. 219, no. 1, pp. 131–141, 2013.
- 903 [36] J. Jing, H. Sun, J. A. Kim, A. Herlopian, I. Karakis, M. Ng, J. J. Halford,  
904 D. Maus, F. Chan, M. Dolatshahi *et al.*, "Development of expert-level  
905 automated detection of epileptiform discharges during electroencephalo-  
906 gram interpretation," *JAMA Neurology*, vol. 77, no. 1, pp. 103–108,  
907 2020.
- 908 [37] B. J. Ruijter, J. Hofmeijer, M. C. Tjepkema-Cloostermans, and M. J.  
909 van Putten, "The prognostic value of discontinuous EEG patterns in  
910 postanoxic coma," *Clinical Neurophysiology*, vol. 129, no. 8, pp. 1534–  
911 1543, 2018.
- 912 [38] S. Bai, J. Z. Kolter, and V. Koltun, "An empirical evaluation of generic  
913 convolutional and recurrent networks for sequence modeling," *arXiv*  
914 *preprint arXiv:1803.01271*, 2018.
- 915 [39] J. A. Hanley and B. J. McNeil, "The meaning and use of the area under  
916 a receiver operating characteristic (ROC) curve," *Radiology*, vol. 143,  
917 no. 1, pp. 29–36, 1982.
- 918 [40] C. Cortes and M. Mohri, "Confidence intervals for the area under  
919 the ROC curve," *Advances in Neural Information Processing Systems*,  
920 vol. 17, pp. 305–312, 2005.
- 921 [41] T. Lin, T. Guo, and K. Aberer, "Hybrid neural networks for learning  
922 the trend in time series," in *International Joint Conference on Artificial*  
923 *Intelligence*, no. CONF, 2017, pp. 2273–2279.
- 924 [42] Y. Roy, H. Banville, I. Albuquerque, A. Gramfort, T. H. Falk, and  
925 J. Faubert, "Deep learning-based electroencephalography analysis: a  
926 systematic review," *Journal of Neural Engineering*, vol. 16, no. 5, p.  
927 051001, 2019.
- 928 [43] R. J. Madathil, R. S. Hira, M. Stoeckl, F. Sterz, J. B. Elrod, and  
929 G. Nichol, "Ischemia reperfusion injury as a modifiable therapeutic  
930 target for cardioprotection or neuroprotection in patients undergoing  
931 cardiopulmonary resuscitation," *Resuscitation*, vol. 105, pp. 85–91,  
932 2016.
- 933 [44] E. Amorim, J. C. Rittenberger, M. E. Baldwin, C. W. Callaway,  
934 A. Popescu, and P. C. A. Service, "Malignant EEG patterns in cardi-  
935 ac arrest patients treated with targeted temperature management who  
936 survive to hospital discharge," *Resuscitation*, vol. 90, pp. 127–132, 2015.
- 937 [45] C. M. Drohan, A. I. Cardi, J. C. Rittenberger, A. Popescu, C. W. Call-  
938 away, M. E. Baldwin, and J. Elmer, "Effect of sedation on quantitative  
939 electroencephalography after cardiac arrest," *Resuscitation*, vol. 124, pp.  
940 132–137, 2018.
- 941 [46] B. J. Ruijter, M. J. van Putten, W. M. van den Bergh, S. C. Tromp, and  
942 J. Hofmeijer, "Propofol does not affect the reliability of early EEG for  
943 outcome prediction of comatose patients after cardiac arrest," *Clinical*  
944 *Neurophysiology*, vol. 130, no. 8, pp. 1263–1270, 2019.
- 945 [47] C. S. Youn, C. W. Callaway, J. C. Rittenberger *et al.*, "Combination of  
946 initial neurologic examination, quantitative brain imaging and electroen-  
947 cephalography to predict outcome after cardiac arrest," *Resuscitation*,  
948 vol. 110, pp. 120–125, 2017.
- 949 [48] M. B. Bevers, B. M. Scirica, K. R. Avery, G. V. Henderson, A. P. Lin,  
950 and J. W. Lee, "Combination of clinical exam, MRI and EEG to predict  
951 outcome following cardiac arrest and targeted temperature management,"  
952 *Neurocritical Care*, vol. 29, no. 3, pp. 396–403, 2018.
- 953 [49] J. H. Kim, M. J. Kim, J. S. You, H. S. Lee, Y. S. Park, I. Park, and  
954 S. P. Chung, "Multimodal approach for neurologic prognostication of  
955 out-of-hospital cardiac arrest patients undergoing targeted temperature  
956 management," *Resuscitation*, vol. 134, pp. 33–40, 2019.
- 957 [50] M. Oddo and A. O. Rossetti, "Early multimodal outcome prediction  
958 after cardiac arrest in patients treated with hypothermia," *Critical Care*  
959 *Medicine*, vol. 42, no. 6, pp. 1340–1347, 2014.
- 960 [51] C. Sandroni, S. D'Arrigo, and J. P. Nolan, "Prognostication after cardiac  
961 arrest," *Critical Care*, vol. 22, no. 1, pp. 1–9, 2018.
- 962 [52] N. Ben-Hamouda, F. S. Taccone, A. O. Rossetti, and M. Oddo, "Con-  
963 temporary approach to neurologic prognostication of coma after cardiac  
964 arrest," *Chest*, vol. 146, no. 5, pp. 1375–1386, 2014.
- 965 [53] A. Esteva, A. Robicquet, B. Ramsundar, V. Kuleshov, M. DePristo,  
966 K. Chou, C. Cui, G. Corrado, S. Thrun, and J. Dean, "A guide to deep  
967 learning in healthcare," *Nature Medicine*, vol. 25, no. 1, pp. 24–29, 2019.
- 968 [54] A. Rajkomar, J. Dean, and I. Kohane, "Machine learning in medicine,"  
969 *New England Journal of Medicine*, vol. 380, no. 14, pp. 1347–1358,  
970 2019.